

Band-gap renormalization of optically excited semiconductor quantum wells

J. C. Ryan and T. L. Reinecke

Naval Research Laboratory, Washington, D.C. 20375

(Received 22 October 1992)

The band-gap renormalization of optically excited semiconductor quantum wells due to exchange-correlation effects in the electron-hole system is studied here. The first-order self-energies for this two-component electron-hole plasma are calculated exactly within the random-phase approximation. All intersubband interactions are included fully, and they are found to make significant contributions to the self-energies and to their subband dependences. Particular attention is paid to the subband dependence of the band-gap renormalization. These calculations are made for realistic systems with finite well widths, finite barrier heights, and finite temperatures. The results are compared with recent experimental data for $\text{In}_x\text{Ga}_{1-x}\text{As}/\text{InP}$ and $\text{GaAs}/\text{Ga}_{1-x}\text{Al}_x\text{As}$ quantum wells.

I. INTRODUCTION

The renormalization of the band gap in semiconductors due to high carrier densities is an important many-body effect that has been studied in bulk systems for some time. This effect is of technological importance in, e.g., diode lasers and optical bistability. It is most often seen under optical excitation when enhanced densities of both free electrons and holes are present. Under these circumstances the band gap is found to decrease with increasing carrier densities due mainly to the exchange-correlation effects in the electron-hole plasma. Recent experimental results on semiconductor quantum-well systems have allowed this effect to be studied for varying dimensionality.¹⁻⁴ Among the most interesting experiments to date are those^{3,4} on $\text{In}_x\text{Ga}_{1-x}\text{As}/\text{InP}$ and $\text{GaAs}/\text{Ga}_{1-x}\text{Al}_x\text{As}$ quantum-well systems which show that the renormalization depends on the subbands involved in the transition.

The band-gap renormalization arises because the self-energies of the band-edge states shift due to Coulomb interactions among free carriers. The local-density approximation (LDA) gives a simple and useful description of these interactions in the ground state of many inhomogeneous systems and has been shown to give a reasonable approximation to the overall band-gap renormalization in quantum-well systems.⁴ Its applicability in quantum-well systems with their rapidly varying densities is not clear, however, and it has been found to underestimate the subband dependence of the renormalizations in them.⁴ In order to obtain a quantitative understanding of the renormalizations and of their subband dependence in quantum-well systems fully dynamic random-phase-approximation (RPA) self-energy calculations are done here. The need to do full self-energy calculations to understand band-gap renormalizations has been pointed out in connection with single carrier modulation-doped quantum wells by Zimmermann *et al.*⁵ In order to make quantitative comparisons with experiment we will show that all intrasubband and intersubband Coulomb interactions for the two-component electron-hole system should be included and that the calculations should be done for

realistic systems with finite well widths, finite barrier heights, and finite temperatures.

Previous work on the band-gap renormalization of optically excited semiconductor quantum wells has been done by several groups⁶⁻⁹ who have employed a number of different approximations. In some of the most recent work, Ell and Haug⁸ used a plasmon-pole approximation for the exchange-correlation shifts. It has been argued⁵ that this approximation is inadequate. This is due to the questionable validity of the plasmon pole approximation for quasi-two-dimensional systems as well as the fact that these authors used a Padé approximation to solve the Dyson equation for the screened Coulomb-interaction matrix and that they neglected the intersubband contributions to the self-energy. Das Sarma, Jalabert, and Yang⁹ have calculated the RPA self-energy at zero temperature for a model system with infinite barrier heights, but they only considered a single electron and single hole subband. Inclusion of the higher subbands can be expected to have a significant effect on the self-energies. In related work, mentioned above, Zimmerman *et al.*⁵ have performed a RPA calculation of the band-gap renormalization of a one-component system in a modulation-doped semiconductor quantum well neglecting only the intersubband interactions.

In the present work we give a complete treatment of the fully dynamical self-energy and the resulting subband-dependent band-gap renormalization in the RPA for a two-component electron-hole system. In particular, no approximations are made in solving for the screened Coulomb-interaction matrix. Also the calculations are made for finite well widths, finite barrier heights, and finite temperatures. Among the important features of this work are the full inclusion of intersubband and intrasubband interactions for the two-component system. We find that the intersubband interactions make significant contributions to the renormalization and in particular to its subband dependence. These results are compared with experimental data and with the results of the LDA.

The formalism for the self-energy calculation in the RPA is given in Sec. II. Numerical results and comparison with experiment are discussed in Sec. III.

II. SELF-ENERGY

The RPA self-energy is the energy of a carrier interacting with itself via the RPA screened Coulomb interaction. In this approach the self-energy of the electron (or hole) is calculated by taking the propagation of the carrier between emission and absorption of the virtual plasmon to be that of a noninteracting particle. In this case for a symmetric quantum well, the first-order self-

energy is diagonal in the subband index so that the renormalized subband edge is given by

$$e_{\alpha}(0) = \epsilon_{\alpha}(0) + \text{Re} \left[\sum_{\alpha} (0, \epsilon_{\alpha}(0)) \right], \quad (1)$$

where the index α refers both to the type of carrier (electron or hole) and the subband index. The RPA self-energy is given by

$$\sum_{\alpha}(\mathbf{q}, i\omega_{\nu}) = - \sum_{\alpha'} \int \frac{d^2k}{4\pi^2} \frac{1}{\beta} \sum_{\nu'} V_{\alpha\alpha', \alpha\alpha'}(\mathbf{q}-\mathbf{k}, i\omega_{\nu} - i\omega_{\nu'}) G_{\alpha'}^0(\mathbf{k}, i\omega_{\nu}), \quad (2)$$

where G^0 is the noninteracting Green's function

$$G_{\alpha}^0(\mathbf{k}, i\omega_{\nu}) = [i\omega_{\nu} - \epsilon_{\alpha}(\mathbf{k})]^{-1}, \quad (3)$$

$\epsilon_{\alpha}(\mathbf{k})$ is the noninteracting subband energy relative to the chemical potential, and the Matsubara frequencies are $\omega_{\nu} = (2\nu+1)\pi/\beta$, $\nu=0, \pm 1, \pm 2, \dots$ and $\beta = (k_B T)^{-1}$. The RPA screened Coulomb interaction (plasmon propagator) obeys the Dyson equation

$$V_{\alpha\alpha', \beta\beta'}(\mathbf{q}, i\omega) = V_{\alpha\alpha', \beta\beta'}^0(\mathbf{q}) + \sum_{\alpha''\beta''} V_{\alpha\alpha'', \beta''\beta}^0(\mathbf{q}) \prod_{\alpha''\beta''}^0(\mathbf{q}, i\omega) V_{\alpha''\alpha', \beta\beta''}(\mathbf{q}, i\omega) \quad (4)$$

with the unscreened Coulomb matrix elements given in terms of the subband envelope functions, $\psi_{\alpha}(z)$, by

$$V_{\alpha\beta, \beta'\alpha'}^0(\mathbf{q}) = \frac{2\pi e^2}{\epsilon_0 q} \int \psi_{\alpha}^*(z) \psi_{\alpha'}(z) \exp[-q|z-z'|] \psi_{\beta}^*(z') \psi_{\beta'}(z') dz dz', \quad (5)$$

where q is the magnitude of the momentum parallel to the quantum well. The noninteracting polarizability is expressed in terms of the noninteracting eigenvalues and the Fermi distribution functions, n_F , as

$$\prod_{\alpha\beta}^0(\mathbf{q}, i\omega) = \int \frac{d^2k}{2\pi^2} \frac{n_F[\epsilon_{\alpha}(\mathbf{k}+\mathbf{q})] - n_F[\epsilon_{\beta}(\mathbf{k})]}{\epsilon_{\alpha}(\mathbf{k}+\mathbf{q}) - \epsilon_{\beta}(\mathbf{k}) - i\omega}. \quad (6)$$

In Eq. (5) the subband indices can be interpreted as a carrier in subband α being scattered into subband α' by a carrier in subband β which is scattered into subband β' . For instance, $V_{00,00}$ is an intrasubband interaction where all carriers remain in subband zero, $V_{01,10}$ is an interaction in which a carrier in subband one scatters off a carrier in subband zero but no intersubband transitions are induced, and $V_{00,11}$ is an intersubband interaction in which both carriers are scattered from subband zero to subband one. Interactions that couple the intersubband and intrasubband modes, such as $V_{01,11}$, are all zero in a symmetric well because the wave functions have definite parity.

In studying the many-body effects due to carrier-carrier interactions in compound semiconductors it has often been found¹⁰ that the dynamical interaction of the

carriers with LO phonons can be represented well by screening the Coulomb interaction with the low-frequency dielectric constant ϵ_0 in the so-called " ϵ_0 approximation." This procedure is used here as seen in Eq. (5).

The frequency sum in Eq. (2) can be performed by using the spectral representation of V ,

$$V_{\alpha\alpha', \beta\beta'}(\mathbf{q}, i\omega) = V_{\alpha\alpha', \beta\beta'}^0(\mathbf{q}) + \int \frac{d\omega'}{\pi} \frac{\text{Im} V_{\alpha\alpha', \beta\beta'}^{\text{ret}}(\mathbf{q}, \omega')}{\omega' - i\omega}, \quad (7)$$

where the retarded version of V is obtained by the analytical continuation $i\omega \rightarrow \omega + i\delta$. The retarded self-energy can then be obtained from the same analytic continuation,

$$\begin{aligned} \sum_{\alpha}(\mathbf{q}, \omega) = & - \sum_{\alpha'} \int \frac{d^2k}{4\pi^2} V_{\alpha\alpha', \alpha\alpha'}(\mathbf{q}-\mathbf{k}, \Delta\epsilon) n_F[\epsilon_{\alpha'}(\mathbf{k})] - \sum_{\alpha'} \int \frac{d^2k}{4\pi^2} [V_{\alpha\alpha', \alpha\alpha'}(\mathbf{q}-\mathbf{k}, \Delta\epsilon) - V_{\alpha\alpha', \alpha\alpha'}^0(\mathbf{q}-\mathbf{k})] n_B[-\Delta\epsilon] \\ & + \sum_{\alpha'} \int \frac{d^2k}{4\pi^2} \frac{1}{\beta} \sum_{\nu} \frac{V_{\alpha\alpha', \alpha\alpha'}(\mathbf{q}-\mathbf{k}, i\omega_{\nu}) - V_{\alpha\alpha', \alpha\alpha'}^0(\mathbf{q}-\mathbf{k})}{i\omega_{\nu} - \Delta\epsilon}, \end{aligned} \quad (8)$$

where $\Delta\epsilon = \omega - \epsilon_{\alpha'}(\mathbf{k})$, and n_B and n_F are the Bose and Fermi distribution functions, respectively.

Use of the above equilibrium formalism in the present case is only possible because each of the components (electrons and holes) can be considered to be in quasiequilibrium. This is because the intraband relaxation rate for the electrons and that for the holes is much greater than the interband recombination/relaxation rate. The noninteracting quasiequilibrium chemical potentials are calculated separately for each type of carrier by assuming a quasi-two-dimensional system of the sheet density, n ($n_e = n_h$), at finite temperature. The quasi-chemical potential of carrier i obeys

$$\exp(\beta\hbar^2\pi n/m_i) = \prod_a (1 + \exp\{\beta[\mu_i - \epsilon_{i,a}(0)]\}), \quad (9)$$

where the product extends over subbands, a , and m_i is the effective mass of carrier i . When only two subbands are considered, a closed form expression for μ is obtained for each type of carrier,

$$\begin{aligned} \mu = & \frac{\epsilon_1(0) + \epsilon_0(0)}{2} \\ & + \frac{1}{\beta} \ln\{[\sinh^2(\beta\epsilon_{10}/2) + \exp(\beta\hbar^2\pi n/m)]^{1/2} \\ & - \cosh(\beta\epsilon_{10}/2)\}, \end{aligned} \quad (10)$$

where $\epsilon_{10} = \epsilon_1(0) - \epsilon_0(0)$.

There are several different names for various combinations of the terms in Eq. (8). The first term is called the screened exchange for obvious reasons, and the last two are the residue and line terms, respectively.¹¹ The sum of the last two terms is also known as the Coulomb-hole self-energy, and it describes the energy of interaction of the electron with the depleted density of surrounding electrons due to exchange and correlation.

For zero temperature the self-energy can be obtained by letting $\beta \rightarrow \infty$. In this limit the sequence of Matsubara frequencies becomes a continuum, and the frequency sum becomes an integral as $1/\beta\sum \rightarrow \int d\omega/2\pi$. \prod^0 can also be integrated analytically at zero temperature. As a practical matter of calculational efficiency we note that the line term contains an integrable singularity since both ω and $\Delta\epsilon$ go through zero. The substitution $\omega = |\Delta\epsilon|\tan\theta$ is found to remove the singularity and also to map the infinite frequency domain to a finite θ domain which gives for the line term in Eq. (8)

$$-\text{sgn}(\Delta\epsilon) \sum_{\alpha'} \int \frac{k dk}{2\pi} \int \frac{d\theta}{\pi} [V_{\alpha\alpha',\alpha\alpha'}(k, i\Delta\epsilon \tan\theta) - V_{\alpha\alpha',\alpha\alpha'}^0(k)]$$

for $0 < \theta < \pi/2$.

III. DISCUSSION

In order to discuss the present results for the band-gap renormalization we have made calculations for a 103-Å GaAs/Ga_{1-x}Al_xAs quantum well for which experimental data are available. First we consider the several contributions at zero temperature. The numerical evalua-

tions begin with the eigenfunctions and eigenvalues of the finite square well, with barrier heights determined separately for electrons and holes.¹² Significant population is found only in the first two electron and first two hole subbands, and therefore only those are included in the calculations. Heavy-hole subbands are included in the parabolic approximation. We have found that the effects of including the light-hole subbands are small (typically ~ 3 meV in the renormalization) because of their higher energy and lower occupation, and therefore they are neglected here. We have also found that the Hartree contributions to the self-energies are small (~ 2 meV). This occurs because the net charge density is nearly zero at all points. The renormalization of the band gap is the sum of the electron and the hole self-energies at the band edges. The quantities of interest here are the density-dependent changes in the 1e-1hh transition (first electron subband to first heavy-hole subband) and in the 2e-2hh transition. The difference between these transition energies is referred to as the "splitting" between them.

We first consider the screened exchange and Coulomb-hole contributions to the renormalization of the band gap. Figure 1 shows this decomposition with the total renormalization at zero temperature. The most obvious point is that the splitting of the renormalization of the two subband transitions is due mainly to the screened exchange. This is because the screened exchange depends upon occupation, and the higher-lying subbands are always less occupied than are the lower ones. The Coulomb-hole contributions, on the other hand, depend upon how effectively the Coulomb field of the particle is screened and are relatively insensitive to the details of the subband occupation. The Coulomb-hole contribution to the splitting of the renormalization is therefore less. The kinks in the curves occur at the points at which the higher subbands begin to fill. At higher temperatures, as will be seen below, these features become thermally smeared.

It is particularly interesting to look at the intersubband and intrasubband contributions separately. Figure 2

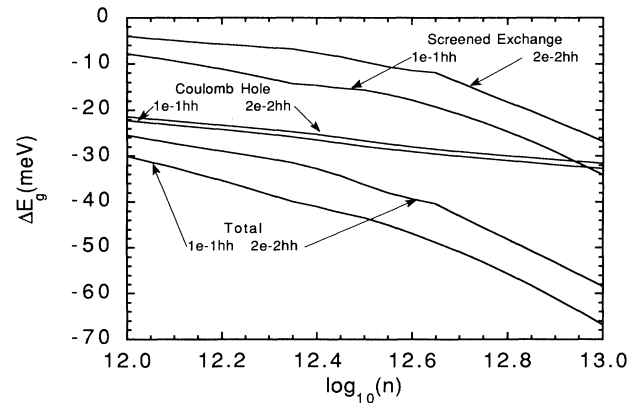


FIG. 1. The screened exchange (dashed lines) and Coulomb-hole (dotted lines) contributions to the band-gap renormalizations and the total renormalizations as functions of density for a 103-Å GaAs/Ga_{1-x}Al_xAs quantum well at zero temperature as a function of electron and hole sheet density n .

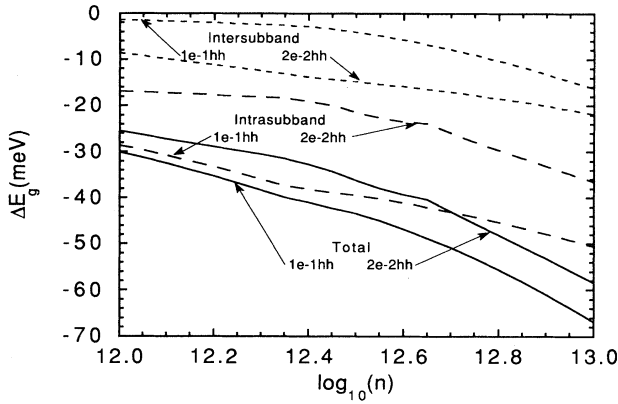


FIG. 2. The intrasubband and intersubband contributions to the band-gap renormalizations of a 103-Å GaAs/Ga_{1-x}Al_xAs quantum well at zero temperature as a function of sheet density n .

shows these terms along with the total renormalization for zero temperature. We see that the magnitude of the intersubband contribution is significant, although somewhat smaller than the intrasubband contribution. The sign of the splitting between the lowest and next-lowest transition is opposite for the intersubband and intrasubband contributions, and therefore the intersubband contribution decreases the splitting between the 1e-1hh and the 2e-2hh renormalizations. This is because the screened exchange is primarily responsible for the splitting and the lowest subband and has the greatest occupancy. Therefore the intersubband screened exchange is greater for the upper subbands, whereas the opposite is true for the intrasubband screened exchange.

We have obtained the renormalizations at finite temperature by performing the Matsubara summations in Eq. (8). Results for the 103-Å GaAs/Ga_{1-x}Al_xAs quantum well are given in Fig. 3. There it is seen that the effects of finite temperature decrease the overall renormalization and decrease the splitting. This behavior results from the increased occupation of higher-lying momentum states and the relative increase of the occupation of the upper subbands at higher temperature.

In the LDA the exchange-correlation interaction is replaced by a local potential which is obtained from bulk results. In the present case we must generalize the LDA to two components, which we do by fitting to bulk calculations for two-component systems. The exchange-correlation potential is given by $v_{xc}^i(\mathbf{r}) = \delta E_{xc}[n_e(\mathbf{r}), n_h(\mathbf{r})] / \delta n_i(\mathbf{r})$, where E_{xc} is the exchange-correlation energy. From calculations for bulk systems it is known that the exchange-correlation energy is to a good approximation independent of the material and band structure provided that the units of length are given by a set of excitonic units appropriate for each material.¹³ In addition, for bulk systems the contributions to the electron and hole self-energies are nearly equal and nearly independent of wave vector.¹⁴ Therefore, we divide the exchange-correlation energy equally between the electrons and holes,

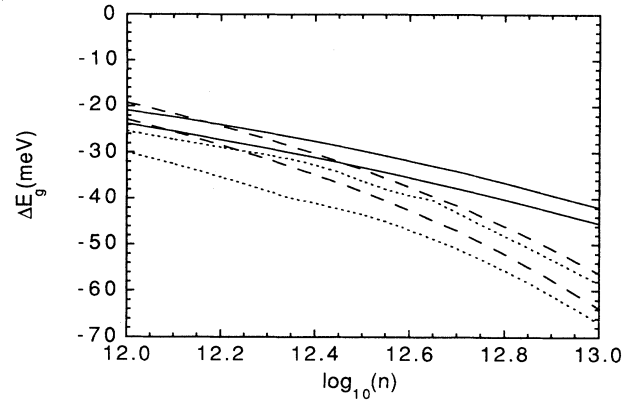


FIG. 3. The band-gap renormalizations of a 103-Å GaAs/Ga_{1-x}Al_xAs quantum well at zero temperature (dotted lines), and at 300 K (dashed lines) as a function of sheet density n from the self-energy calculations in the text. The solid lines give the results of the local-density approximation at 300 K described in the text. In each case the lower curve corresponds to the transition between the lowest electron and lowest heavy-hole subband and the upper curve corresponds to the second electron subband to second heavy-hole subband transition.

$$E_{xc}[n_e(\mathbf{r}), n_h(\mathbf{r})] = \frac{1}{2} \int [n_e(\mathbf{r})\epsilon_{xc}(n_e(\mathbf{r})) + n_h(\mathbf{r})\epsilon_{xc}(n_h(\mathbf{r}))] d\mathbf{r}, \quad (11)$$

where ϵ_{xc} is the exchange-correlation energy per electron-hole pair. We have fit ϵ_{xc} to the detailed results for two-component bulk systems.¹³ For the density dependence we use a form like that suggested by Hedin and Lundquist¹⁵ and obtain

$$v_{xc}^i(r_s^i) = -2[1 + B(r_s^i/A)\ln(1 + A/r_s^i)] / \pi\alpha r_s^i, \quad (12)$$

where $i=e, h$, $\alpha=(4\pi/9)^{1/3}$, and r_s^i is given by $n_i a_x^3 = 4\pi(r_s^i)^3/3$ for each component. We obtain $A=21$ and $B=1.89$. The unit of energy is the excitonic Rydberg $e^2/(2\epsilon_0 a_x)$, where the unit of length is the excitonic Bohr radius $a_x = \hbar^2 \epsilon_0 / e^2 \mu$. Here μ is the optical mass $\mu^{-1} = m_e^{-1} + m_h^{-1}$, where m_e, m_h are the electron and hole masses.

Results obtained from self-consistent LDA calculations are shown in Fig. 3 for the case of the 103-Å GaAs/Ga_{1-x}Al_xAs quantum well at 300 K. Bulk values of band parameters are used in these calculations, and the densities are taken to be the total densities. It is seen that the overall magnitude of the renormalization in the LDA is somewhat less than that of the self-energy calculations, the density dependence is less strong, and that the splitting between the transitions for the different subbands is less. In the LDA the splitting between the subbands arises from the different spatial dependences of the total charge density in the different subbands, and it does not take into account the different occupation of the subbands. Thus the LDA should not give as complete an account of the subband dependence of the band-gap renormalization as do the self-energy calculations.

We have also made two modifications in this simple LDA which permit it to account better for the band-gap

renormalization of quantum-well systems.^{4,16} By using an exciton Rydberg and an exciton Bohr radius appropriate for the quantum-well system, we find⁴ that the overall magnitude is in better agreement with experiment. This procedure is motivated by scaling with energy and length units as done in bulk systems.¹³ In addition, by calculating the renormalization of each subband in terms of the occupancy of that subband alone the splitting of the subband renormalizations is represented better.⁴ This modification is motivated by the subband dependence of the screened exchange found in the present calculations. These modifications produce a simple and useful way of estimating the band-gap renormalizations and splittings in quantum-well systems.

We compare the present theoretical results from the full self-energy calculations with the recent high-density photoluminescence data of Lach *et al.*⁴ on GaAs/Ga_{0.63}Al_{0.37}As quantum wells at 300 K and those of Kulakovskii *et al.*^{3,17} for In_{0.53}Ga_{0.47}As/InP quantum wells at 77 K. These experiments were made using mesa structures in order to obtain high uniform carrier densities. They were analyzed using detailed line-shape fits which included the full valence-band nonparabolicity. The comparison of experiment and theory for a 103-Å GaAs quantum well is shown in Fig. 4 and comparisons for In_xGa_{1-x}As quantum wells of 80-, 150-, and 190-Å widths are shown in Figs. 5(a)–5(c). The kink remains in the theoretical results at 77 K because the thermal energy is small compared to the subband separations, whereas at 300 K the curves are smoother.

From these results it is seen that the overall magnitude of the renormalizations is in reasonably good agreement with experiment. The subband splitting, however, is not in quantitative agreement with experiment, and the deviations are seen to vary from system to system. For example, the agreement is quite good for the 80-Å In_xGa_{1-x}As quantum well and less good for wider quan-

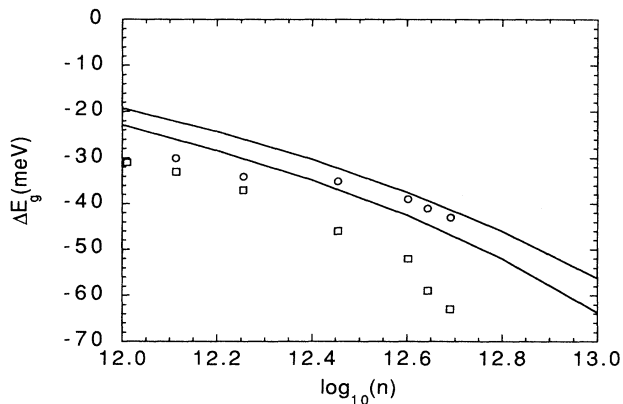


FIG. 4. The theoretical results (solid lines) for the band-gap renormalizations of a 103-Å GaAs/Ga_{1-x}Al_xAs quantum well at 300 K compared to the experimental results of Lach *et al.* (Ref. 4). The lower curve and squares are for the transition between the lowest electron and lowest heavy-hole subbands, and the upper curve and circles are for the second electron subband to second heavy-hole subband transition.

tum wells where the theoretical results give decreasing splitting with increasing well widths. The reason that the theoretical splittings are greater for narrower wells is that the narrower wells have larger intersubband energy separations which decrease the intersubband Coulomb interactions. The total splitting between the transitions is decreased by the intersubband contributions, and there-

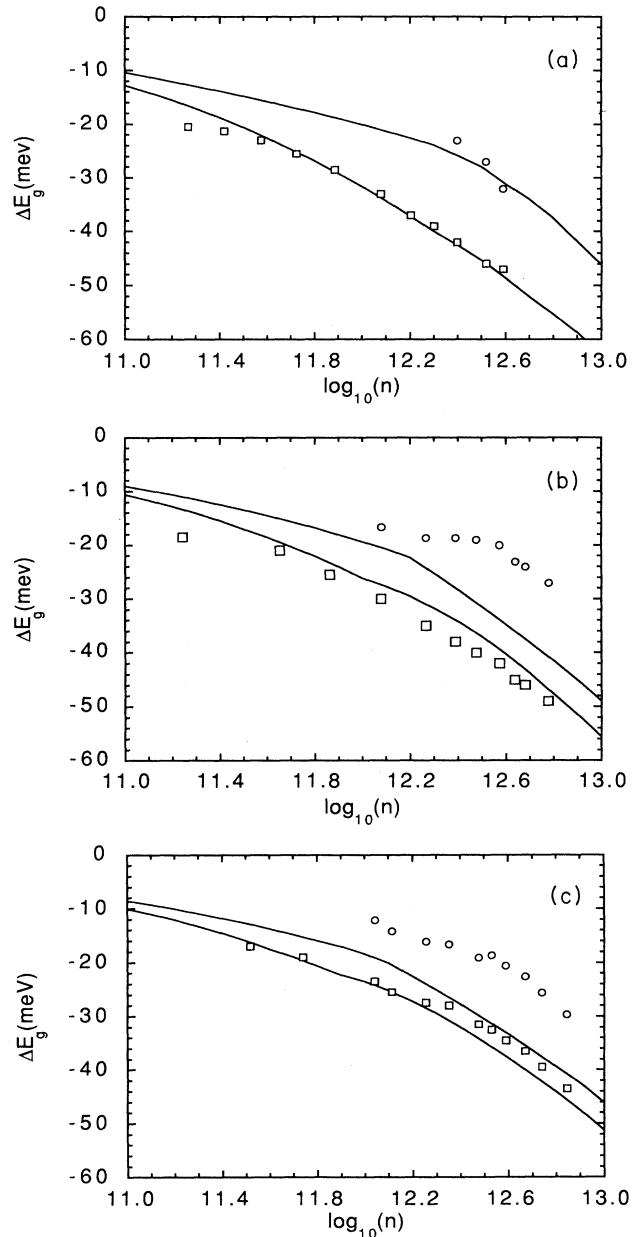


FIG. 5. Theoretical results (solid lines) for the band-gap renormalizations of In_xGa_{1-x}As/InP quantum wells at 77 K compared with the experimental results of Kulakovskii *et al.* (Refs. 3 and 17) for (a) 80-Å well width, (b) 150-Å well width, and (c) 190-Å well width. The lower curves and squares correspond to the lowest electron to heavy-hole transition, and the upper curves and circles to the second electron subband to second heavy-hole subband transition.

fore the splittings are greater for narrower wells.

Vertex corrections are not included in the RPA. These corrections may play an important role in lower-dimensional systems. In the present work they are expected to increase the intersubband energy separation by the depolarization shift, which will increase the renormalization splittings. We also note that the full nonparabolicity of the valence bands has not been taken into account in these calculations, but we do not expect this feature to have a large effect on the theoretical results because they are not strongly dependent on details of the band structure. Finally we note that there may be considerable uncertainty in the experimental results because

they are obtained from multiparameter fits to photoluminescence spectra for the temperature, subband densities, and subband renormalizations. This may account in part for the varying quality of the comparisons between theory and experiment in the different systems.

ACKNOWLEDGMENTS

This work was supported in part by the Office of Naval Research and the National Research Council. One of us (T.L.R.) is grateful to A. Forchel for many helpful conversations concerning the experimental results.

¹G. Traenkle, H. Leier, A. Forchel, H. Haug, C. Ell, and G. Weimann, *Phys. Rev. Lett.* **58**, 419 (1987).

²K.-H. Schlaad *et al.*, *Phys. Rev. B* **43**, 4268 (1991).

³V. D. Kulakovskii, E. Lach, A. Forchel, and D. Gruetzmacher, *Phys. Rev. B* **40**, 8087 (1989).

⁴E. Lach, A. Forchel, D. A. Broido, T. L. Reinecke, G. Weimann, and W. Schlapp, *Phys. Rev. B* **42**, 5395 (1990).

⁵R. Zimmermann, E. H. Böttcher, N. Kirstaedtr, and D. Bimberg, *Superlatt. Microstruct.* **7**, 433 (1990).

⁶S. Schmitt-Rink, C. Ell, S. W. Koch, H. E. Schmidt, and H. Haug, *Solid State Commun.* **52**, 123 (1984).

⁷G. E. Bauer and T. Ando, *J. Phys. C* **19**, 1537 (1986).

⁸C. Ell and H. Haug, *Phys. Status Solidi B* **159**, 117 (1990).

⁹S. Das Sarma, R. Jalabert, and S. -R. Eric Yang, *Phys. Rev. B* **39**, 5516 (1989); **41**, 8288 (1990).

¹⁰G. Beni and T. M. Rice, *Phys. Rev. B* **18**, 768 (1978).

¹¹J. J. Quinn and R. A. Ferrell, *Phys. Rev.* **112**, 812 (1958).

¹²For the GaAs/Ga_{1-x}Al_xAs system the electron and heavy-hole masses in GaAs were taken to be 0.0665 and 0.378 and in

Ga_{0.63}Al_{0.37}As were 0.079 and 0.36, the conduction- and valence-band offsets were taken to be 300 and 161 meV, and the dielectric constant in GaAs was taken to be 12.35. For the In_xGa_{1-x}As/InP system the electron and heavy-hole masses in In_{0.53}Ga_{0.47}As were taken to be 0.041 and 0.377 and in InP were 0.07 and 0.40, the conduction- and valence-band offsets were taken to be 202 and 490 meV, and the dielectric constant in In_{0.53}Ga_{0.47}As was taken to be 13.9.

¹³P. Vashishta and R. K. Kalia, *Phys. Rev. B* **25**, 6492 (1982).

¹⁴T. M. Rice, in *Solid State Physics*, edited by F. Seitz, D. Turnbull, and H. Ehrenreich (Academic, New York, 1977), Vol. 32.

¹⁵L. Hedin and B. I. Lundquist, *J. Phys. C* **4**, 2064 (1971).

¹⁶T. L. Reinecke, D. A. Broido, E. Lach, V. Kulakovskii, A. Forchel, and D. Gruetzmacher, *Superlatt. Microstruct.* **7**, 437 (1990).

¹⁷V. D. Kulakovskii, E. Lach, A. Forchel, D. A. Broido, T. L. Reinecke, and D. Gruetzmacher (private communication).